

# Systematic Delineation of a Calmodulin Peptide Interaction

Claus Hultschig<sup>1</sup>, Hans-Jürgen Hecht<sup>2</sup> and Ronald Frank<sup>1\*</sup>

<sup>1</sup>Department of Chemical Biology of the GBF (German Research Centre for Biotechnology), Mascheroder Weg 1, D-38124 Braunschweig Germany

<sup>2</sup>Department of Structural Biology of the GBF (German Research Centre for Biotechnology), Mascheroder Weg 1, D-38124 Braunschweig Germany

We present a comprehensive profile of amino acid side-chain constraints in a calmodulin (CaM) peptide complex. These data were obtained from the analysis of calmodulin binding to an array of all single substitution analogues as well as N- and C-terminal truncations of the skMLCK derived M13 peptide ligand. The experimentally derived binding data were evaluated with respect to the known 3D-structure of the CaM/M13 complex. Besides an almost perfect agreement between the measured affinities and the structural data, the unexpected high-affine Asn5Ala variant of the M13\* peptide described by Montigiani *et al.* could be verified. In contrast to other reports our data clearly support the postulate of the minor and major hydrophobic anchors of this calcium dependent interaction.

© 2004 Elsevier Ltd. All rights reserved.

**Keywords:** SPOT synthesis; protein–peptide interaction; calmodulin; peptide array; structure activity relationship

\*Corresponding author

## Introduction

Calmodulin (CaM) is a small acidic ubiquitous protein and conserved extraordinarily throughout the evolution of eukaryotes. Essentially all vertebrates contain identical calmodulins, even though encoded by different genes.<sup>1,2</sup> CaM is an integral modulator of many calcium-dependent processes in virtually every eukaryotic cell-type. It functions as a cytosolic calcium receptor and binds four calcium ions with very high affinity. In this way it responds to a variety of different extra cellular signals which increase the cytosolic calcium level.<sup>3,4</sup> Thereby Calmodulin decodes the Ca<sup>2+</sup> signal that is brought about by the influx of Ca<sup>2+</sup> through respective

Ca-channels in the plasma membrane<sup>5</sup> and activates or deactivates both kinases and phosphatases. Furthermore, calmodulin regulates enzymes involved in the signal transduction such as cyclic nucleotide phosphodiesterases, adenylate cyclases, nitric oxide synthetase and plasma membrane calcium ATPases. There are, however, protein families including neuromodulin, myosin, ion-channels that bind calmodulin at remarkably low concentrations or even in the absence of calcium.<sup>3,6</sup>

Upon loading the four calcium-binding sites with calcium ions, a conformational change in calmodulin is rapidly induced<sup>7</sup> resulting in the exposition of hydrophobic patches on the surface of calmodulin,<sup>8</sup> which enable the protein to bind to a variety of different target proteins with extraordinary high affinity. A number of organic hydrophobic molecules such as derivatives of naphthalene<sup>9</sup> and natural peptides such as peptide hormones, neurotransmitters and venoms also bind calmodulin with high affinity.<sup>3</sup>

The binding to target proteins or peptides results in further major structural changes as revealed by the structure of the complex between calmodulin and the CaM binding site (M13 peptide) of skeletal muscle myosin light chain kinase (skMLCK). The structure is shown in Figure 1(b) and (c) and was first solved by Ikura *et al.*<sup>10</sup> The central  $\alpha$ -helix, showing a high thermal motion in the uncomplexed state of calmodulin (Figure 1(a)), turns into a linker connecting both domains of calmodulin in a very

Present address: Claus Hultschig, Max-Planck Institute für Molekulare Genetik, Abteilung Lehrach/AG Automation, Ihnestr. 73, D-14195 Berlin, Germany.

Abbreviations used: C20W, peptide LRRGQILWFRGLNRIQTQIK; C24W, peptide QILWFRGLNRIQTQIRVVNAFRSS; cam, gene encoding for CaM; CaM, calmodulin (protein); M13, 26-mer CaM binding region of rabbit skeletal myosin light chain kinase; M13\*, central 19 AA of the M13 peptide in contract with CaM as described by Ikura *et al.*; M13\*(Arg5Ala), a point mutant of M13\* in which Arg5 is substituted by Ala first as described by Montigiani *et al.*; PEG, polyethyleneglycol; roi, region of interest; smMLCK, smooth muscle myosin light chain kinase.

E-mail address of the corresponding author: frank@gbf.de

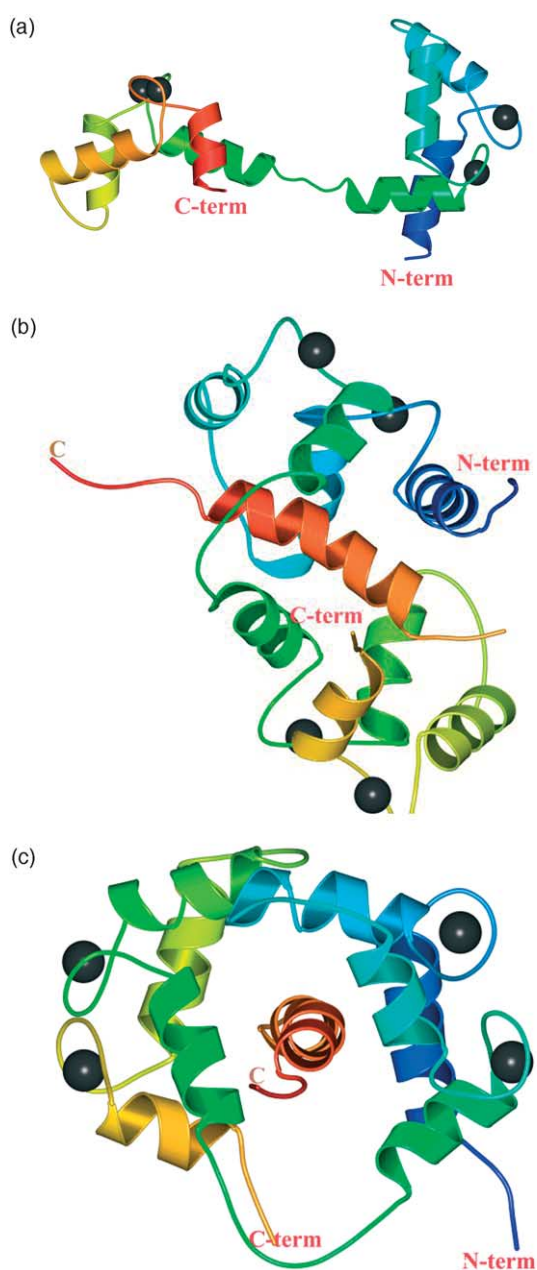


**Figure 1.** Ribbon diagrams illustrating the structure of calcium loaded calmodulin (a) and calcium loaded calmodulin bound the CaM binding region of skeletal muscle myosin light chain kinase (b) and (c). The significant structural rearrangements in calmodulin upon binding to its target can be derived. Figure 1(a) is based on the pdb file 3clm.<sup>27</sup> Figure 1(b) and (c) is derived from the pdb file 2BBM.<sup>10</sup> The drawings were generated by using programs *MOLSCRIPT*<sup>28</sup> and rendered with *gl\_renderer* (Esser & Deisenhofer, unpublished program) and *POVRAY*<sup>TM</sup>.

flexible manner. Due to this flexible linker both domains of calcium-loaded calmodulin are able to engulf the target peptide. Calmodulin wraps itself literally around the peptide. Upon binding of calmodulin to the skMLCK peptide the two domains of calmodulin approach the central flexible loop

and form a hydrophobic arch by coalescing wide hydrophobic patches from both domains. The different hydrophobic patches of both domains can be arranged due to the flexibility of the linker so that both patches of CaM oppose different hydrophobic sides of the  $\alpha$ -helical complexed peptide.

In sharp contrast to the high degree of conservation of calmodulin throughout evolution, the different calmodulin target protein sites and peptides seem to share little homology in their primary structure.<sup>11</sup> So far, no clear consensus for the CaM binding sites could be derived. Most of these calcium dependent CaM binding sequences, however, contain a region that is characterized by a basic, often amphipathic helix of approximately 20 amino acid residues. A few of them are shown in Table 1. There are critical hydrophobic residues at position 1 and 14 (commonly referred to as the main hydrophobic anchors), as well as at positions 5 and 8 (the minor hydrophobic anchors). Tryptophan residues are sometimes present but are not essential. Basic amino acid residues are distributed throughout the motif and often flank the critical hydrophobic residues.<sup>6</sup>

Montigiani *et al.*<sup>12</sup> have studied the remarkably stable (3.7 nM) complex of CaM and the M13 peptide in more detail with a set of synthetic peptides representing a systematic alanine scan of the ligand peptide sequence. The authors found a peptide mutant having a significantly increased affinity for CaM. In this mutant an asparagine at position 5 is substituted by an alanine. However, the importance of none of the hydrophobic anchors could be derived from this study.

More recently, Bosc *et al.*<sup>13</sup> have presented an investigation of the CaM regulated activity of the STOP protein in tubulin stabilization. In this report, several CaM binding sites were identified which all were functional and included low affinity sites that had only very little or no homology to a CaM consensus. Thus, a deeper understanding of the structural features of CaM binding sites is required to reliably recognize such important regulatory features of proteins. This prompted us to disclose our comprehensive study of the CaM/M13-peptide complex using an array of 425 synthetic peptides on a cellulose membrane<sup>14</sup> representing all point mutants and selected truncation variants of the M13 peptide.

## Results and Discussion

Previous work of Ikura *et al.*<sup>10</sup> showed that a central 19-mer of the parent M13 peptide (Table 1) is in contact with CaM. Accordingly, we have chosen this 19 mer RWKKNFIAVSAANRFKKIS (M13<sup>\*</sup>) and its Asn5Ala mutant (M13<sup>\*</sup>(Asn5Ala))<sup>12</sup> for a more detailed investigation.

To allow for a systematic and comprehensive analysis of the influence of amino acid residues to CaM binding affinity we have screened all 342 single replacement analogues (cysteine excluded) of

**Table 1.** Summary of several amino acid sequences of calmodulin binding peptides and protein target sites in part adopted from Crivici & Ikura.<sup>3</sup>

SkMLCK (M13)	K R R <b>W</b> K K N <b>F</b> I A <b>V</b> S A A N <b>R</b> <b>F</b> K K I S S
smMLCK	A R R K <b>W</b> Q K T G H A <b>V</b> R A I G <b>R</b> L S S
CaMK II	A R R K <b>L</b> K G A <b>I</b> L T T M <b>L</b> A T <b>R</b> N F S
Caldesmon	G <b>V</b> R N I K S M <b>W</b> E K G N V <b>F</b> S S
Calspermin	A R R K <b>L</b> K A A <b>V</b> K A <b>V</b> V A S S <b>R</b> L G S
PFK	F M N N W E V <b>Y</b> K L L <b>A</b> H I R P P A P <b>K</b> S G S Y T V
Calcineurin	A R K E V <b>I</b> R N K <b>I</b> R A <b>I</b> G K M A <b>R</b> <b>V</b> F S V L R
Ca <sup>2+</sup> ATPase	R G Q I L <b>W</b> F R G <b>L</b> N R <b>I</b> Q T Q I <b>K</b> <b>V</b> V N A F S
PDE	R R K H <b>L</b> Q R P <b>I</b> F R <b>L</b> R C L V <b>K</b> Q L E K
NOS	K R R A I G <b>F</b> K K L <b>A</b> E A <b>V</b> K F S A <b>K</b> L M G Q
Neurom.	K A H K A A T K <b>I</b> Q A S <b>F</b> R G H I T R K <b>K</b> L K G E K K
Spektrin	K T A S P <b>W</b> K S A R L M <b>V</b> H T V A T <b>F</b> N S I K E
MARKS	K K K K R <b>F</b> S F K K S F K L S G F S <b>F</b> K K S K K
Mastoparan	<b>I</b> N L K <b>A</b> L A <b>A</b> L A K K I <b>L</b>
Mellitin	G I G G A V <b>L</b> K V L T T G <b>L</b> P A L I S <b>W</b> I K R K R

The sequences are aligned by visual inspection of the putatively conserved major hydrophobic anchors, marked in bold and blue, and minor hydrophobic anchors marked in bold and green. Further criteria for the alignment are the putatively conserved basic residues, which are marked in black and bold. These basic residues were found in two calmodulin peptide structure<sup>19,20</sup> to be essential for the binding of CaM to these peptides. The hydrophobic anchors interact with hydrophobic patches of calmodulin in the structures published.<sup>10,19,20</sup>

the M13\* peptide. In addition the importance of the hydrophobic anchors was also addressed by a series of truncation variants. All together, a corresponding array of 425 peptides including also 24 copies of the wild-type M13\* peptide was chemically synthesized by the SPOT method.<sup>14</sup> This peptide array was used directly in a parallel solid phase binding assay to obtain the affinities of calmodulin for this set of peptides relative to the wild-type M13\* peptide.

### Design and application of the peptide array

Four hundred and twenty-five different peptide spots were synthesized by SPOT synthesis on a amino-PEG-modified cellulose membrane of 8 cm × 12 cm in size. The peptides were arranged in 25 columns and 17 rows (Figure 2). In the first row (Spots 1–25) truncated variants of the M13\* peptide were synthesized as listed in Figure 3(a), left side, whereas in the 17th row (Spots 401–425) the same set of truncations for the M13\* (Asn5Ala) peptide were synthesized (Figure 3(a), right side). Spots no. 26–386 represent the replacement set of the M13\* peptide in which every amino acid of the M-13\* is substituted serially by all genetically encoded L-amino acid residues, with the exception of cysteine.

This array was probed with <sup>35</sup>S labeled CaM obtained by coupled *in vitro* transcription–translation from the cam-coding DNA under control of the T7 promoter. The autoradiograph of the <sup>35</sup>S-CaM binding in the presence of 5 mM CaCl<sub>2</sub> is shown in Figure 2. To correct for calcium independent and unspecific binding, CaM was dissociated with EDTA and the remaining radioactivity was detected by autoradiography (not shown). The numerical intensities of all spots are provided in the supplementary information. The M13\* peptide is included 24 times on this array and the binding of <sup>35</sup>S-CaM to this peptide was reproducible with a

standard deviation ( $\sigma_n$ ) of only 21% which is very good with respect to a synthesis process of almost 40 consecutive steps per peptide.

Figure 3(a) and (b) summarizes the relative peptide–calmodulin affinities in a graphical representation. These will be discussed in detail below in the context of characteristic features of CaM–target interactions as summarized in the introduction. Both primary amino acid sequence features and the published NMR structure (2BBM)<sup>10</sup> were considered for understanding the experimentally observed preferences. All peptide–CaM complexes were also modeled with program O<sup>15</sup> and visually

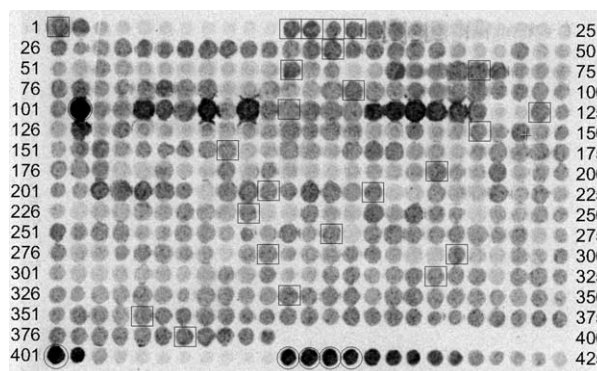


**Figure 2.** Autoradiograph of <sup>35</sup>S-CaM binding to peptides derived from the central 19 mer-CaM binding site of rabbit skeletal muscle myosin light chain kinase (M13\* peptide).<sup>10</sup> Peptides 1–25 represent C- and N-terminal truncation series of the M13\* peptide (see Figure 3(a)). No. 26–386 represent the analogue study of this peptide (see Figure 3(b)), whereas peptides 401–425 represent a series of C- and N-terminal truncated peptides derived from a point mutant of the M13\* peptide, the M13\*(Arg5Ala)<sup>12</sup> (see Figure 3(a)). <sup>35</sup>S-CaM binding was detected with multipurpose phosphorimaging screens. Image contrast settings: 50–1500 counts. Copies of the M13\* peptide are boxed and copies of the M13\*(Arg5Ala) mutant are circled.

(a)

M-13* truncation series	norm Intensity	norm Intensity	M-13* (Asn5Ala) series
RWKKNFIAVSAANRFKKIS	100	429	RWKKAFIAVSAANRFKKIS
WKKNFIAVSAANRFKKIS	134	373	WKKA <del>F</del> IAVSAANRFKKIS
KKNFIAVSAANRFKKIS	24	42	KKAFIAVSAANRFKKIS
KNFIAVSAANRFKKIS	12	13	KAFIAVSAANRFKKIS
NFIAVSAANRFKKIS	8	9	AFIAVSAANRFKKIS
FIAVSAANRFKKIS	9	5	FIAVSAANRFKKIS
IAVSAANRFKKIS	4	4	IAVSAANRFKKIS
AVSAANRFKKIS	5	4	AVSAANRFKKIS
VSAANRFKKIS	4	3	VSAANRFKKIS
SAANRFKKIS	4	3	SAANRFKKIS
AANRFKKIS	1	4	AANRFKKIS
RWKKNFIAVSAANRFKKI	97	309	RWKKAFIAVSAANRFKKI
RWKKNFIAVSAANRFKK	102	277	RWKKAFIAVSAANRFKK
RWKKNFIAVSAANRFK	64	277	RWKKAFIAVSAANRFK
RWKKNFIAVSAANRF	26	188	RWKKAFIAVSAANRF
RWKKNFIAVSAANR	13	147	RWKKAFIAVSAANR
RWKKNFIAVSAAN	12	62	RWKKAFIAVSAAN
RWKKNFIAVSAA	6	48	RWKKAFIAVSAA
RWKKNFIAVSA	6	34	RWKKAFIAVSA
RWKKNFIAVS	7	29	RWKKAFIAVS
RWKKNFIAV	6	14	RWKKAFIAV

(b)

	1	2	3	4	5	6	7	8	9	10	11	12	13	14	15	16	17	18	19
	R	W	K	K	N	F	I	A	V	S	A	A	N	R	F	K	K	I	S
A	90	28	52	91	429	134	97	100	75	130	100	100	79	91	42	90	70	71	98
D	53	13	14	26	87	20	48	31	20	44	20	20	45	26	21	37	54	40	67
E	49	12	22	40	94	18	58	47	19	75	23	21	58	52	19	41	41	71	56
F	67	45	130	48	270	100	132	82	70	63	50	82	73	95	100	74	61	108	80
G	97	14	88	50	180	56	48	76	21	75	35	53	70	44	19	95	69	77	76
H	81	15	74	36	139	43	59	44	18	59	23	27	42	44	18	45	54	54	63
I	114	32	95	58	337	325	100	96	71	158	83	146	85	76	51	65	50	100	83
K	95	18	100	100	75	46	64	154	21	169	29	51	50	101	22	100	100	96	65
L	96	50	100	67	258	124	138	118	71	195	64	138	95	92	69	82	73	104	82
M	74	28	41	64	106	68	54	65	26	141	26	89	55	69	36	67	79	95	74
N	73	19	35	108	100	46	77	68	20	106	26	65	100	63	23	68	87	100	70
P	59	19	26	80	112	27	43	33	13	14	13	13	13	17	16	25	44	94	70
Q	97	16	73	75	88	85	126	76	23	108	29	48	90	74	23	69	74	100	68
R	100	15	112	92	72	46	131	79	34	120	27	36	94	100	25	62	91	97	99
S	93	17	52	67	300	72	60	79	26	100	56	55	83	64	31	66	62	103	100
T	87	15	64	70	307	66	86	102	44	108	44	56	65	63	22	75	67	78	96
V	83	20	75	49	295	115	88	86	100	180	70	128	81	70	34	45	55	120	116
W	77	100	124	37	207	101	111	74	44	108	43	78	56	88	62	40	48	100	79
Y	68	37	66	72	186	97	82	77	32	71	32	79	53	98	33	50	39	113	103

**Figure 3.** Normalized presentations of  $^{35}\text{S}$ -CaM binding data for variants of the M13\* peptide shown in Figure 2. Relative intensities of the spots were calculated by first correcting for the non-dissociable radioactivity after washing with EDTA and then normalization by setting the wild-type M13\* peptide to 100%. For the M13\* and the M13\*(Asn5Ala) peptide the average signal intensities of the multiple copies are used. Colors of the cells indicate: red for <60%; yellow for 60% to 140%; green for >140% of bound calmodulin relative to wild-type peptide (boxed). Thresholds are based on twice the standard deviation from the wild-type peptide. (a) N- and C-terminal truncation series of the M13\* and M13\*(Arg5Ala) respectively. (b) Replacement analogues of peptide spots 26–386 shown in Figure 2.

inspected for agreement with the affinity data. The fit of the resulting modeled mutant peptides to calmodulin was evaluated for all major conformers of each amino acid introduced. The standard major conformers are based on a proposal of Kleywegt & Jones.<sup>16</sup> Those authors evaluated the side-chain conformations of all amino acid residues in crystallographically determined protein structures deposited in the protein data bank. The major conformers identified by those authors are incorporated in a databank of program *O*.

### Truncation analysis of the M13\* peptide and the M13\*(Asn5Ala) peptide

Figure 3(a) shows the corrected normalized affinities of the truncation series from both peptide variants. The N-terminal Arg 1 could be removed without any notable reduction in the affinity. The removal of tryptophan 2, the first main hydrophobic anchor, and all subsequent amino acid residues led to a dramatic decrease ( $\sim 80\%$ ) of the affinity of CaM for the resulting peptides. This is a strong indication for the importance of this particular residue for the stability of the CaM–M13 complex. For the peptides derived by C-terminal truncation, a continued decrease in the affinity of CaM for the resulting peptides was observed even beyond the second main hydrophobic anchor (Phe15). This can be rationalized from the different structures described by Ikura *et al.*,<sup>10</sup> which were calculated on the basis of the interatomic distances determined by NMR. Those different structures are averaged to give the pdb file 2BBM. The possible different structures of M13 within the CaM–M13 complex are shown in Figure 4. Essentially all these structures are postulated to be present in solution. The positioning of the N terminus of the M13 peptide is rather fixed in the different structures, whereas the positioning of the C terminus varies significantly. This disordering of the  $\alpha$ -helix at the C terminus of the  $\text{Ca}^{2+}$ -CaM bound peptide implies that the second main hydrophobic anchor is not as tightly bound as the Trp2, the first main hydrophobic anchor, and hence less crucial for binding. Exactly these features are confirmed by both series of truncation peptides.

Possibly, the weak binding shorter c-terminal peptides form a different complex than the full length peptide in the 2BBM structure. Kataoka *et al.*<sup>17</sup> found significant differences in the shapes of two CaM–peptide complexes, observed with solution X-ray scattering. For the complex of  $\text{Ca}^{2+}$ -CaM and a peptide having both main hydrophobic anchors separated by 12 amino acid residues (C24W) a close globular structure is observed. In contrast, the complex of  $\text{Ca}^{2+}$ -CaM and a truncated peptide lacking the C terminus up to the main hydrophobic anchor (C20W), an extended non-globular shape is described. This is similar to a non peptide-complexed calcium loaded CaM, suggesting an interaction of this truncated peptide with only one lobe of CaM.

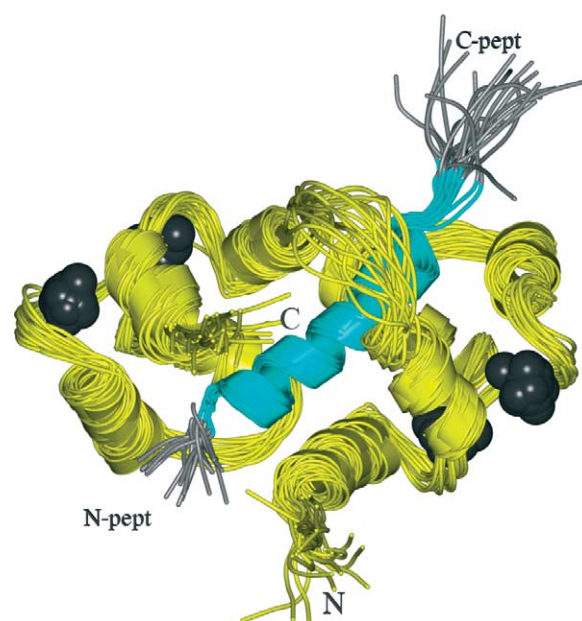


**Figure 4.** Superposition of the different possible, NMR derived, positions of the M13 peptide (shown in grey) within the CaM–M13 complex. CaM is shown in yellow,  $\text{Ca}^{2+}$  ions are shown in black. The N terminus of the complexed peptide is marked N-pept; it is located for all likely structures at a similar position. The position of the C terminus, marked C-pept, varies significantly for the different likely structures. N and C mark the N and C terminus of calmodulin in the complex. The part of the complexed peptide analysed in detail in this study (M13\*) is highlighted in cyan.

### Analogue analysis of the M13\* peptide

Figure 3(b) illustrates the corrected normalized affinities of the analogue study. Significant changes in affinity for CaM in comparison to the wild-type peptide are highlighted by red and green colors. We will discuss the affects of mutations at each position in the peptide sequence. A corresponding series of pictures showing the local environment of each amino acid of the wild-type peptide in the complex is provided in the online supplementary information.

Arg1 was already identified above for being not crucial for the overall stability of the CaM–M13\* complex. Consistently, this amino acid could be replaced by any other residue with only minor effects on the stability of this complex except for acidic side-chains (see below).

Trp2 could not be replaced without significant loss in binding. In place of Trp at position 2 only Leu and Phe were able to maintain CaM affinity to approximately 50% of the wild-type level. This demonstrates again the importance of this position as the first major hydrophobic anchor. This is easily understood because Trp 2 is perfectly embedded in a large hydrophobic pocket of CaM consisting of Phe 89, Phe 92, Ile 100, Met 109, Val 121, Met 124, Ile 125, Val 136, Phe 141, Met 144 and Met 145 as seen in

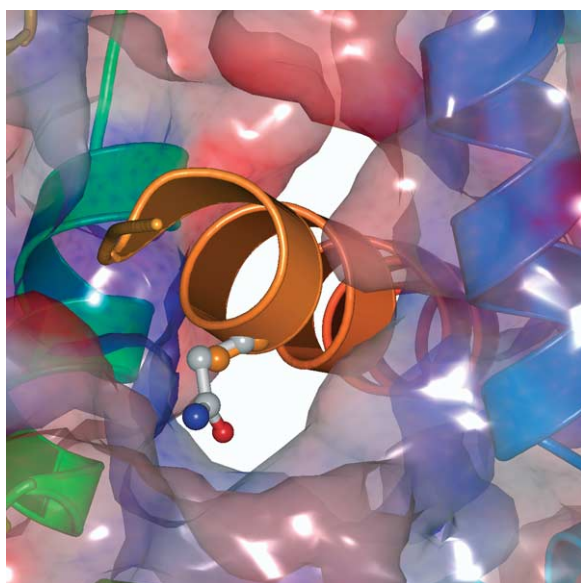


**Figure 5.** Schematic illustration of the Asn5Ala substitution on the basis of the CaM–M13 complex.<sup>10</sup> The large polar side-chain of Asn5 is shown to be in direct vicinity of the hydrophobic pocket of CaM. The carbon atoms of the Asn5 side-chain are shown in gray, the oxygen and the nitrogen atoms of the side-chain amide function are shown in red and blue. The much smaller Ala is shown in orange. The drawing was generated by using program *MOLSCRIPT*<sup>28</sup> and rendered with *gl\_render* (Esser & Deisenhofer, unpublished program) and *POVRAY*<sup>TM</sup>. Coloring of the CaM surface was performed as described by Nicholls,<sup>29</sup> hydrophobic patches of the CaM surface are marked in blue, and red indicates a polar environment.

the NMR structure. (2BBM).<sup>10</sup> Any change in a perfect assembly of this type must result in a decreased affinity.

At position 3 and 4, again, acidic residues are most unfavorable for the formation of the corresponding CaM–peptide complex. As for position 1 (Arg), this indicates the overall preference of CaM for basic peptides as reflected in the frequent observation of basic residues flanking the critical hydrophobic anchor residues<sup>6</sup> and may assist in positioning the ligand relative to the acidic entry and exit of the CaM binding channel.<sup>18</sup>

The best binders were found among peptides with substitutions at position 5 (spots 102–120, column 5 in Figure 3(b)). Peptide no. 102, the strongest binder found in this series and also in the whole array, is a peptide obtained by substituting Asn 5 by Ala. This mutant has been already described by Montigiani *et al.*,<sup>12</sup> who performed an alanine scan with the M13 peptide. CaM affinity of these mutants reveals a clear preference for amino acid residues with small hydrophobic side-chains: Ala is by far the best fitting and Ile the second best. Amino acid residues with long aliphatic side-chains such as asparagine, glutamine, lysine, arginine, and methionine were less favorable.

The findings described above are in good agreement with the structure of the M13–CaM complex.<sup>10</sup> The environment of Asn 5 in the CaM–M13 complex was analyzed with program *O* and is illustrated in Figure 5. The responsible hydrophobic pocket in CaM consisting of Phe 92, Val 108, Met 109, Leu 112, and Leu 116 accommodating Asn 5 is rather small and formed in a way that more space filling polar side-chains simply do not fit or cannot adopt a conformation fitting to this cavity. Our detailed analysis confirms the interpretation of Montigiani *et al.*<sup>12</sup> that the parent Asn 5 side-chain is unfavorable and thus its replacement leads in most cases to an increase in peptide CaM affinities.

The hydrophobic pocket for Phe 6, consisting of Ile 85, Ala 88, Phe 89, Phe 92, Phe 141, and Met 145, is located towards one end of the peptide-binding channel and made up of side-chains belonging only to the C-terminal domain of CaM. According to the NMR structure (2BBM),<sup>10</sup> Phe 6 is not perfectly adopted to the hydrophobic cavity. Accordingly the substitution of Phe 6 should be possible. The introduction of Ile results in a threefold improvement of the CaM binding. Figure 6 illustrates the substitution of Phe 6 by Ile. Whereas Phe 6 is not perfectly arranged in the hydrophobic pocket, Ile can adopt itself in a perfect manner to the cavity with one of its major rotamers. The improvement of the CaM binding resulting from the substitution of Phe 6 by Ile can be understood on structural basis in an excellent manner.

Neither the peptide array nor the structural analysis identified a side-chain preference for

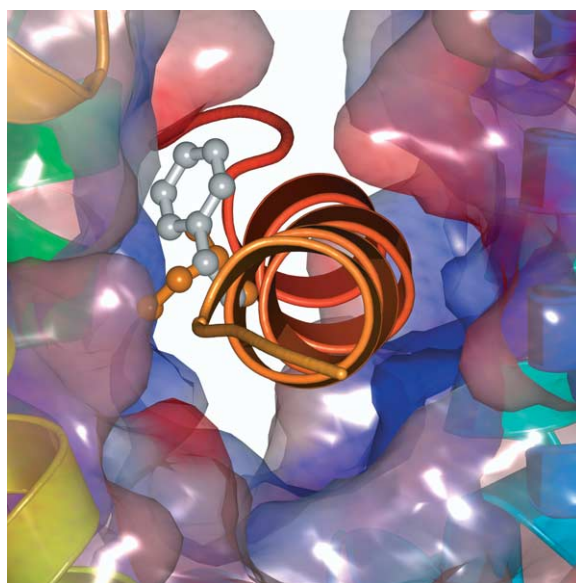


**Figure 6.** Schematic illustration of the Phe6Ile substitution on the basis of the CaM–M13 complex. The Phe6, marked in gray, is shown in the orientation that was found in the NMR measurements of the complex. The Ile at position 6, resulting in an increased affinity of this mutant peptide to CaM, is shown in orange. Given is the manually selected best fitting major rotamer of Ile at position 6. The illustration was generated in the same fashion as Figure 5.

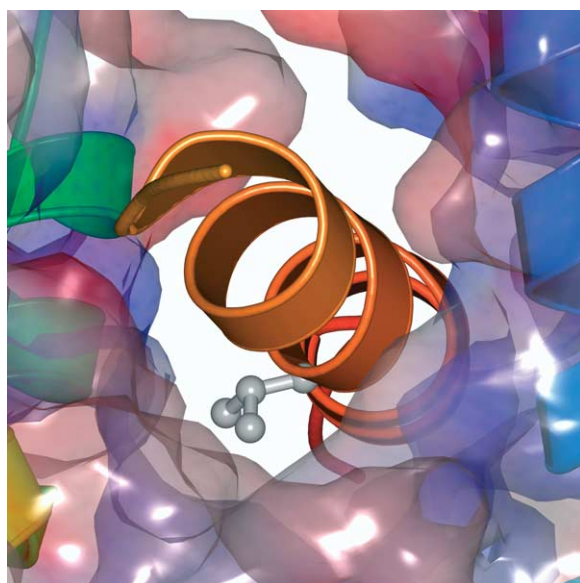


**Figure 7.** Schematic drawing showing the perfect embedding of Val 9 in the hydrophobic pocket of CaM. The direct vicinity of the Val side-chain, which is marked in grey, to the “wall” of the hydrophobic pocket is seen. This implies a steric hindrance of any substitution of Val 9 by more space filling amino acid residues. The illustration was generated in the same fashion as Figure 5.

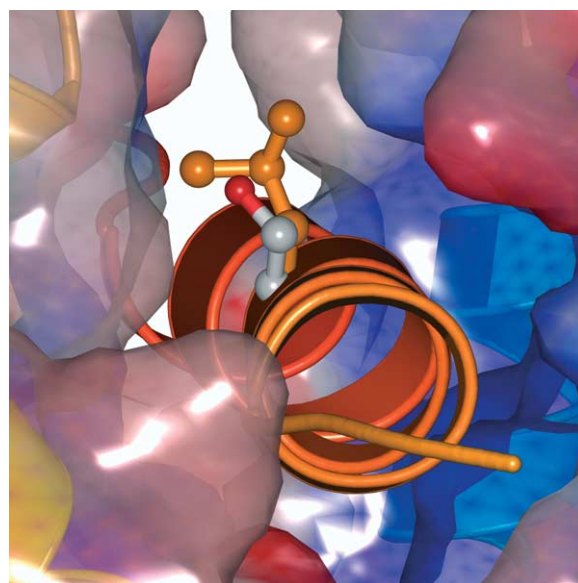


**Figure 8.** Schematic illustration showing the substitution of Ser 10 by Leu. The improvement in the binding can be understood with respect to the hydrophobic environment of Ser 10, which is shown in gray and red. The illustrated Leu rotamer, which is marked in orange, fits perfectly to this environment and was manually selected from the pool of different major rotamers. The illustration was generated in the same fashion as Figure 5.

position 7. For the next position, the substitution of Ala 8 by Lys resulted in a clear improvement in the CaM binding by 50%. This cannot be derived from the structure of the CaM–M13 complex: there is no acidic residue at a suitable distance available to form an ionic interaction and most rotamers of Lys tested at position eight with program O should be unfavorable due to steric hindrance. Only one Lys rotamer avoids steric clashes but contributes only hydrophobic side-chain interactions.

Val 9 cannot be substituted by any other amino acid without decreasing the CaM binding capability. This decrease is less pronounced for the other hydrophobic residues, which is in good agreement with the concept of a second hydrophobic anchor. Val 9 is located in a hydrophobic pocket made up from both CaM domains. This pocket consists of Ala 88, Val 91, Phe 92, Val 108, Leu 112, Phe 19, Val 35 and Leu 39 and forms a perfect hydrophobic shield for Val 9 (Figure 7).

Ser 10 tolerates almost all substitutions except the helix breaking proline and the acidic residues (see below). In particular, flexible side-chains can be accommodated in the channel formed by both hydrophobic patches of CaM for this position. A major rotamer of Val fits perfectly to this environment as illustrated in Figure 8.

At position 11 the peptide array data reveal a clear preference for small hydrophobic aliphatic residues with Ala being the best. A similar but less stringent behavior is found for position Ala 12. Here, however, the other small hydrophobic aliphatic residues show increased affinity.

In contrast, the two following positions, Asn 13 and Arg 14, are particularly tolerant to substitutions except again to proline. In the wild-type peptide both form electrostatic interactions to Glu 84 of CaM. Asn 13 is also involved in hydrophobic contacts and thus flexible hydrophobic residues can adopt to this environment. The tolerance to replacements is particularly surprising for position Arg 14, because this seems to be a conserved residue among many CaM targets (Tab 1) and is thought to stabilize the bent conformation of CaM.<sup>19,20</sup> However, for all residues except His a major rotamer can fit to the adjacent hydrophobic pocket accommodating the second major hydrophobic anchor (Phe 15).

Changes at Phe 15, the position of the second hydrophobic anchor, are generally negative but at least tolerated for Leu, Trp, and Ile. This reduction of the affinity for CaM can be understood with respect to the structural data as well. Phe 15 is perfectly embedded in a hydrophobic pocket consisting of Ile 27, Leu 32, Met 36, Met 51, Ile 52, Val 55, Ile 63, Phe 68, and Met 71 (NMR structure, 2BBM).<sup>10</sup> Any changes in this arrangement will result in a decreased binding capability.<sup>10,18</sup> This situation is very similar to what is observed at position Trp 2 and thus confirms the postulated second hydrophobic anchor crucial for CaM binding.

Lys 16 to Ser 19 comprise the flexible c-terminal tail of the CaM bound peptide. Beyond the second hydrophobic anchor, the influence of amino acid

side-chains on the complex stability gradually diminishes, the same trend as observed in the truncation series.

The global effect of one type of amino acid residue on the overall stability of the complex, usually referred to as "amino acid scans", can be derived from our interaction matrix (refer to Figure 3(b)) when comparing data in horizontal lines. The first line in Figure 3(b) resumes the alanine scan experiment of Montigiani *et al.*<sup>12</sup> The data of these authors do not support the postulate of hydrophobic anchors. However, the alanine scan included in this study is in good agreement with at least the postulate of two major hydrophobic anchors. Because substitution by an alanine is a rather conservative exchange with respect to hydrophobic interactions, the importance of the minor hydrophobic anchors is somewhat obscured. The contribution of these positions becomes more apparent in the glycine scan (Line G), but becomes definitely evident when inspecting the full set of replacements at the respective positions (columns 2, 6, 9, and 15).

Another obvious feature is the consistent negative impact of acidic residues (lines D and E of Figure 3(b)). This agrees well with the basic nature of most calcium dependent CaM targets.<sup>6</sup> Surprisingly the introduction of histidine is for most positions of the M13\* peptide unfavorable. In part, this can be explained by the unfavorable effect of a positive charge resulting from the protonation of His at pH 7 and accounts for those positions where also Lys and Arg are unfavorable (Pos. 2, 6, 9, 11, 12, 13, 15). Careful inspection of the other positions revealed a lack of suitable major rotamers of His, whereas the more flexible Arg and Lys could fit well to perfect (Ala 8).

The introduction of proline, an  $\alpha$ -helix breaking amino acid, at most positions of the M13\* peptide results in a strong decrease of the CaM affinity for the resulting mutant as seen from line P in Figure 3(b). This emphasizes the importance of the  $\alpha$ -helical content of the CaM complexed peptide.<sup>21</sup> Apparently, the helix breaking effect of Pro is most significant for positions 6–17. The N-terminal first turn of the helix is less disturbed by Pro and thus the effects observed accounts more for the particular side-chain interactions.

## Conclusion

We have applied synthetic peptide array technology to systematically explore the high affinity and low sequence specificity of calmodulin binding to its target proteins. The peptide array allowed a convenient comprehensive survey of all 342 single substitution analogues plus two series of N- and C-terminal truncations of a 19 mer peptide ligand M13\*. This study provides the full experimental data set to many theoretical publications of the past ten years. The experimentally observed pattern of peptide CaM complex affinities was in excellent agreement with predictions derived from the NMR

solution structure of the M13–CaM complex using program O. Previously drawn rules for CaM target selection which point at helical nature, at major and minor hydrophobic anchor positions as well as at basic residue positions within the peptide ligand could be questioned with our data set. This clearly supports the important role of the hydrophobic anchor residues (placed +4, +7, and +13 relative to the first one) in an helical structure of the peptide ligand. Other residues discussed to be essential for complex stability as deduced from the solution structure were surprisingly replaceable with a broad range of other amino acid residues. This could be rationalized, however, by alternative modes of interactions.

Calmodulin with its highly promiscuous target selection is a particular challenging case and lends itself to be studied with modern large scale screening methods. Our peptide array approach proved to give reliable information. Further research will include other targets for CaM and also calcium independent ligands. With these studies we will contribute to a better understanding of the structural requirements for calmodulin target recognition and the application of this knowledge to the genome/proteome analysis of cellular regulation pathways involving calcium and calmodulin.

## Material and Methods

All chemicals used were of analytical grade. Aqueous solutions were prepared with double deionized (Milli Q) water. Working buffers were prepared according to standard protocols;<sup>22</sup> where applicable, solutions were autoclaved. Fmoc derivatives of amino acid residues and further reagents for peptide synthesis were obtained from Bachem, Bubendorf, Switzerland; Calbiochem, Bad Soden, Germany, and Alexis, Grünberg, Germany. Free, soluble peptides were synthesized, unless stated otherwise, as N-terminal acylated carboxamides according to standard Fmoc-chemistry<sup>23</sup> with an Abimed AMS222 Multiple Peptide Synthesizer using Tenta GelS resin (Rapp Polymere, Germany) and purified by HPLC. The purity of all peptides used was determined with analytical HPLC and their molecular masses were verified by MALDI-MS (matrix assisted laser desorption ionization mass spectroscopy). Spot synthesis was performed as described<sup>24</sup> with an Abimed ASP222 automated SPOT robot using novel hydrolytically stable amino-PEG-cellulose membranes (AIMS Scientific Products GmbH, Braunschweig, Germany) as a solid support. All coupling reactions were monitored with the bromophenol blue assay and reached completion.

<sup>35</sup>S-CaM was produced *in vitro* using the plasmid pETCaM (a generous gift of Prof. Dr Thomas Grundström and Dr Stefan Herman, Umea University, Sweden) and the Promega TNT<sup>®</sup> coupled transcription/translation system<sup>25</sup> according to the recommendations of the supplier. The formation of calmodulin was verified *via* SDS gel electrophoresis, autoradiography, and silver staining. Fifty microliters of the crude *in vitro* synthesized protein were added to 10 ml of 2× Membrane Blocking buffer (Sigma-Genosys) supplemented with 5 mM CaCl<sub>2</sub> and mixed thoroughly by inverting the tube ten times. This mixture was



applied directly to an spot membrane<sup>26</sup> previously blocked overnight. The incubation was carried out for three hours under constant slow horizontal agitation. The supernatant was removed and the membrane was washed three times for ten minutes with 1× blocking buffer containing 5 mM CaCl<sub>2</sub>, placed on a transparency, and wrapped in saran. The bound <sup>35</sup>S labeled CaM was detected with Molecular Dynamics multi-purpose storage screens, which were always erased prior to their use, placed for 70 hours on top of the saran covered face of the spot membrane, and read out on a Molecular Dynamics Storm 860 (pixel size: 100 μm). The resulting image file was directly imported into the Phoretix ARRAY software (Non Linear Dynamics, UK). For a quantification of the individual spots a suitable grid was chosen in which the diameter of all regions of interest did not exceed the diameter of the smallest spot ( $d=8$  pixel, for scans with pixel sizes of 100 μm). For all scans a rectangle background correction was applied with the rectangle defining the background intensity placed on the membrane in a region outside the spot array. After exposure to the imaging screen, the calcium dependency of the CaM binding was verified by incubating the membrane three times for ten minutes with 1× blocking buffer containing 5 mM EDTA. An image of the remaining radioactivity was obtained as above and used to correct for unspecific binding.

## Acknowledgements

The authors like to thank Prof. Dr Thomas Grundström and Dr Stefan Herman, Umea University, Sweden for the plasmid pETCaM. We thank S. Daenicke for technical assistance in peptide array synthesis. We furthermore appreciate the help and discussions of Dr Peter Röttgen (Affimed Therapeutics AG, Germany), Dr Bernd Haase (Affymetrix, Germany), and Dr Michael Tesar (Morphsys AG, Germany).

## Supplementary Data

Supplementary data associated with this article can be found, in the online version, at [doi:10.1016/j.jmb.2004.08.012](https://doi.org/10.1016/j.jmb.2004.08.012)

## References

- Rhoads, A. R. & Friedberg, F. (1997). Sequence motifs for calmodulin recognition. *FASEB J.* **11**, 331–340.
- Wylie, D. C. & Vanaman, T. C. (1988). Structure and evolution of the calmodulin family of calcium regulatory proteins. In *Calmodulin* (Cohen, P. & Klee, C. B., eds), vol. 5, pp. 1–15, Elsevier Science, Amsterdam.
- Crivici, A. & Ikura, M. (1996). Molecular and structural basis of target recognition by calmodulin. *Annu. Rev. Biophys. Biomol. Struct.* **24**, 85–116.
- Vogel, H. J. (1994). The Merck Frosst Award Lecture 1994. Calmodulin: a versatile calcium mediator protein. *Biochem. Cell. Biol.* **72**, 357–376.
- James, P., Vorherr, T. & Carafoli, E. (1995). Calmodulin-binding domains: just two faced or multi-faceted? *Trends Biochem. Sci.* **20**, 38–42.
- Bähler, M. & Rhoads, A. (2002). Calmodulin signaling via the IQ motif. *FEBS Letters*, **513**, 107–113.
- Bayley, P. M., Findlay, W. A. & Martin, S. R. (1996). Target recognition by calmodulin: dissecting the kinetics and affinity of interaction using short peptide sequences. *Protein Sci.* **5**, 1215–1228.
- Finn, B. E., Evenas, J., Drakenberg, T., Waltho, J. P., Thulin, E. & Forsen, S. (1995). Calcium-induced structural changes and domain autonomy in calmodulin. *Nature Struct. Biol.* **2**, 777–783.
- Osawa, M., Swindells, M. B., Tanikawa, J., Tanaka, T., Mase, T., Furuya, T. & Ikura, M. (1998). Solution structure of calmodulin-W-7 complex: the basis of diversity in molecular recognition. *J. Mol. Biol.* **276**, 165–176.
- Ikura, M., Clore, G. M., Gronenborn, A. M., Zhu, G., Klee, C. B. & Bax, A. (1992). Solution structure of a calmodulin-target peptide complex by multidimensional NMR. *Science*, **256**, 632–638.
- Wilkinson, A. J. (1996). Accommodating structurally diverse peptides in proteins. *Chem. Biol.* **3**, 519–524.
- Montigiani, S., Neri, G., Neri, P. & Neri, D. (1996). Alanine substitutions in calmodulin-binding peptides result in unexpected affinity enhancement. *J. Mol. Biol.* **258**, 6–13.
- Bosc, C., Frank, R., Denarier, E., Ronjat, M., Schweitzer, A., Wehland, J. & Job, D. (2001). Identification of novel bifunctional calmodulin-binding and microtubule-stabilizing motifs in STOP proteins. *J. Biol. Chem.* **276**, 30904–30913.
- Frank, R. (1992). Spot-synthesis: an easy technique for the positionally addressable, parallel chemical synthesis on a membrane support. *Tetrahedron*, **48**, 9217–9232.
- Jones, T. A., Zou, J. Y., Cowan, S. W. & Kjeldgaard, M. (1991). Improved methods for binding protein models in electron density maps and the location of errors in these models. *Acta Crystallog. sect. A*, **47**, 110–119.
- Kleywegt, G. J. & Jones, T. A. (1998). Databases in protein crystallography. *Acta Crystallog. sect. D. Biol. Crystallog.* **54**, 1119–1131.
- Kataoka, M., Head, J. F., Vorherr, T., Krebs, J. & Carafoli, E. (1991). Small-angle X-ray scattering study of calmodulin bound to two peptides corresponding to parts of the calmodulin-binding domain of the plasma membrane Ca<sup>2+</sup> pump. *Biochemistry*, **30**, 6247–6251.
- Afshar, M., Caves, L. S., Guimard, L., Hubbard, R. E., Calas, B., Grassy, G. & Haiech, J. (1994). Investigating the high affinity and low sequence specificity of calmodulin binding to its targets. *J. Mol. Biol.* **244**, 554–571.
- Meador, W. E., Means, A. R. & Quioco, F. A. (1992). Target enzyme recognition by calmodulin: 2.4 Å structure of a calmodulin-peptide complex. *Science*, **257**, 1251–1255.
- Meador, W. E., Means, A. R. & Quioco, F. A. (1993). Modulation of calmodulin plasticity in molecular recognition on the basis of X-ray structures. *Science*, **262**, 1718–1721.
- O'Neil, K. T. & DeGrado, W. F. (1990). How calmodulin binds its targets: sequence independent recognition of amphiphilic alpha-helices. *Trends Biochem. Sci.* **15**, 59–64.
- Sambrook, J., Fritsch, E. F. & Maniatis, T., eds (1989).

- Molecular Cloning: A Laboratory Manual*, 2nd edit., vols. 3, Cold Spring Harbor Laboratory, Cold Spring Harbor, NY.
23. Fields, G. B. & Noble, R. L. (1990). Solid phase synthesis utilizing 9-fluorenylmethoxy-carbonyl amino acids. *Int. J. Peptide Protein Res.* **35**, 161–214.
  24. Frank, R. & Overwin, H. (1996). SPOT synthesis. Epitope analysis with arrays of synthetic peptides prepared on cellulose membranes. *Methods Mol. Biol.* **66**, 149–169.
  25. DiDonato, J. A. & Karin, M. (1993). Co-expression of multiple NF-KB subunits using the TNT<sup>®</sup> System. *Promega Notes*, **42**, 18.
  26. Niebuhr, K. & Wehland, J. (1997). Screening antibody epitopes and regions of protein–protein interaction sites using SPOT peptides. *Immunol. Methods Man.*, 797–800.
  27. Babu, Y. S., Bugg, C. E. & Cook, W. J. (1988). Structure of calmodulin refined at 2.2 Å resolution. *J. Mol. Biol.* **204**, 191–204.
  28. Kraulis, P. J. (1991). MOLSCRIPT: a program to produce both detailed and schematic plots of protein structures. *J. Appl. Crystallog.* **24**, 946–950.
  29. Nicholls, A.J. (1993). GRASP: graphical representation and analysis of surface properties. Columbia University, NY; USA.

*Edited by P. Wright*

*(Received 17 July 2004; accepted 5 August 2004)*